ISSN (Print) 1226-1750
ISSN (Online) 2233-6656
Journal of Magnetics 28(3), 323-330 (2023) https://doi.org/10.4283/JMAG.2023.28.3.323

A Design of Magnetic Resonant Wireless Power Transfer System using Flexible Resonator Coils

Manh Kha Hoang[1,*], Xuan Thuc Kieu[1], Xuan Thanh Pham[1], Trung Kien Vu[1], and Thanh Son Pham[2]

[1]*Faculty of Electronics Engineering, Hanoi University of Industry, Hanoi 10000, Vietnam*
[2]*Institute of Materials Science, Vietnam Academy of Science and Technology, 18 Hoang Quoc Viet, Cau Giay, Hanoi, Vietnam*

(Received 24 March 2023, Received in final form 14 September 2023, Accepted 18 September 2023)

This paper presents a design of magnetic resonant wireless power transfer (MR-WPT) system operating at 6.78 MHz with flexible resonator coils. The resonator coils are fabricated on an FR-4 substrate with a very thin thickness of 0.2 mm; therefore, they can be bent at various angles. With the bendable resonator coils, the configuration of the MR-WPT system will be more flexible, thereby increasing the applicability. However, the inductance, resistance, quality factor, and mutual inductance of the coils will be changed with the bending angle, thereby affecting the performance of the MR-WPT system. Detailed investigations of these changes were conducted by both simulation and experiment. Thus MR-WPT systems with flexible resonators can be designed for optimum performance. This proposed MR-WPT system can be applied in situations where system configuration requires high flexibility. Moreover, a bent resonator system can perform better than a flat resonator system in the inward bending configuration.

Keywords : magnetic resonant wireless power transfer, flexible wireless power transfer, magnetic coupling resonance, bending coil

1. Introduction

The number of electrical and electronic devices is increasing exponentially in modern life. Especially mobile devices such as smartphones and smartwatches have been closely attached to human lives. With the increase in electronic devices, powering them becomes confusing and complicated. Wireless power transfer (WPT) technology provides a solution to that problem. It makes the electric system simple and effective, increasing aesthetics and convenience [1-5].

WPT is a technology that permits the transmission of electrical energy without wires as a physical link [6]. Electrical energy can be transmitted wirelessly in various ways. At long distances, the energy from the transmitting antenna can be transferred to the receiving antenna via far-field radiation [7]. These WPT systems have the advantage of very long transmission distances and are suitable for both information and energy transmission [8]. The efficiency gain of this process is quite small and is only suitable for special applications such as satellites or small power applications. At closer distances, near-field magnetic coupling provides a greater transmission power and no emission of hazardous electromagnetic radiation [9, 10]. Magnetic energy is generally less harmful to humans and the surrounding environment than far-field radiation [11].

Research on magnetic resonant wireless power transfer (MR-WPT) has been widely deployed over the years [12-14]. Its operating principle can be explained by coupled-mode-theory [15]. The inductance of the resonant coils and the mutual inductance between them play an important role in determining the system's performance [16, 17]. In addition, other values, such as the loss with pure resistance and the quality factor (Q-factor) of the resonators, are also factors affecting the system [18]. Many studies have been done to understand the relationship of the system performance to the configuration, size, and environment in which the resonant coils are located [19-21].

In many practical applications, WPT system designs with flat transceivers cannot be used [22, 23]. With various configurations of electrical devices, the transmitting and receiving surfaces can take on many different shapes [24-26]. To increase the applicability of the WPT system,

*Corresponding author: Tel: +84-243-765-5121
Fax: +84-243-765-5261, e-mail: khahoang@haui.edu.vn

studies on their transmission ability when the transceivers are bent were carried out [27-32]. However, an in-depth analysis of how the inductance, mutual inductance, and Q-factor of the resonator are changed when bending, thereby affecting the performance of the WPT system, has not been conducted yet.

In this paper, we propose a design of an MR-WPT system with flexible resonator coils to increase the system's applicability. Detailed and complete studies of resonator coils in various bending conditions have been conducted by both simulation and experiment. The parameters of the resonator coil, such as inductance, resistance, and Q-factor, are investigated with bending angles from 0^o to 90^o. The mutual inductances of two resonator coils at different bending angles for inward and outward configurations are also presented. The efficiency of the WPT system improves from 60.5 % to 75.2 % in the inward bending configuration while degrading from 60 % to 20.5 % in the outward bending configuration. The measured performance of the WPT system is consistent with the coil's characteristics in bending achieved from the analysis.

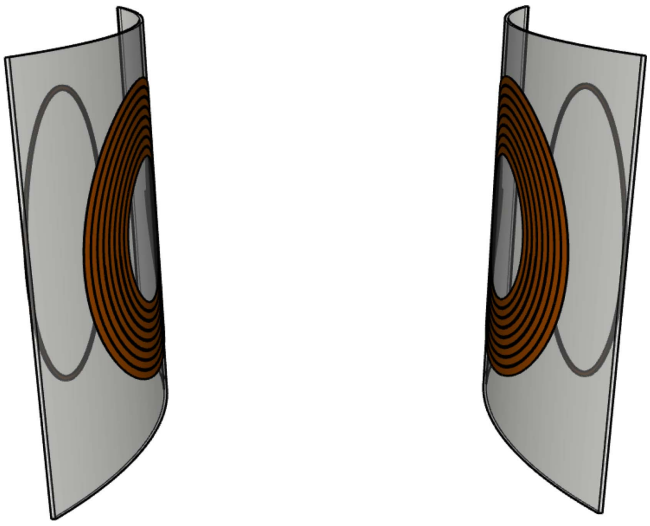

Fig. 1. (Color online) Schematic of the WPT system with flexible resonator coils.

2. Design and Analysis of Flexible Magnetic Resonant Wireless Power Transfer

Figure 1 illustrates the configuration of the proposed MR-WPT system with bendable resonator coils. The MR-WPT system has a 4-coil construction with a source loop, transmitter resonator (Tx), receiver resonator (Tx), and receiver loop. The two resonators have the same design with a spiral shape and operate at 6.78 MHz. The distance between the Tx and the Rx coil $d_{\text{Tx-Rx}}$ is 200 mm. The resonator coils are bendable to increase flexibility, thereby increasing the applicability of the MR-WPT system. The Tx/Rx has an outer diameter of 145 mm, and the source/load loop has a diameter of 120 mm.

In MR-WPT systems, the spiral coil structure loaded with an external capacitor is a model with many advantages for designing a resonator coil. Figure 2(a) depicts the resonator coil of WPT system by an 8-turn spiral resonator loaded with a lumped capacitor. The resonator is fabricated on a thin FR-4 substrate with a thickness of 0.2 mm and a dielectric constant of 4.3. The thickness of the copper layer on the FR-4 substrate is 0.07 mm. The spiral has a strip width W = 5 mm, spacing between strip S = 0.5 mm, and the outer radius R_{out} 145 mm. The total size of the resonator is D = 160 mm. Two ends of the resonator are connected to the back panel through two vias from which an external capacitor can be soldered to the spiral on the back side of the structure. The resonant frequency of the resonator can be controlled by changing the capacitor value. To make the WPT system operate at 6.78 MHz, a capacitor of 150 pF was used. Thanks to their very thin thickness, the resonator coils can be easily bent to various curvatures. Therefore, it can increase the applicability of

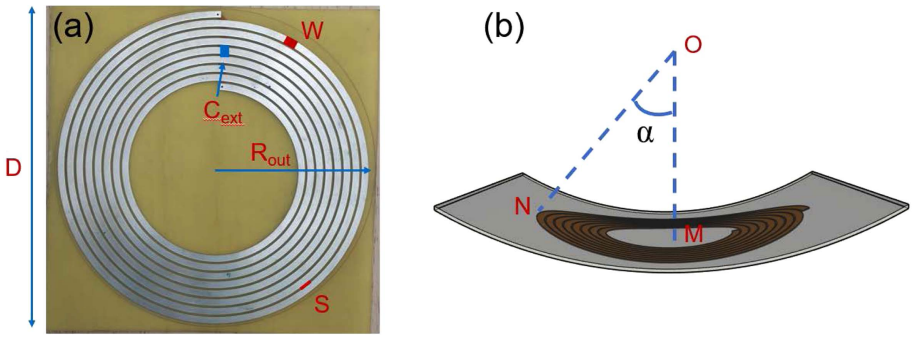

Fig. 2. (Color online) (a) Design of resonator coil, (b) schematic of bending resonator coil.

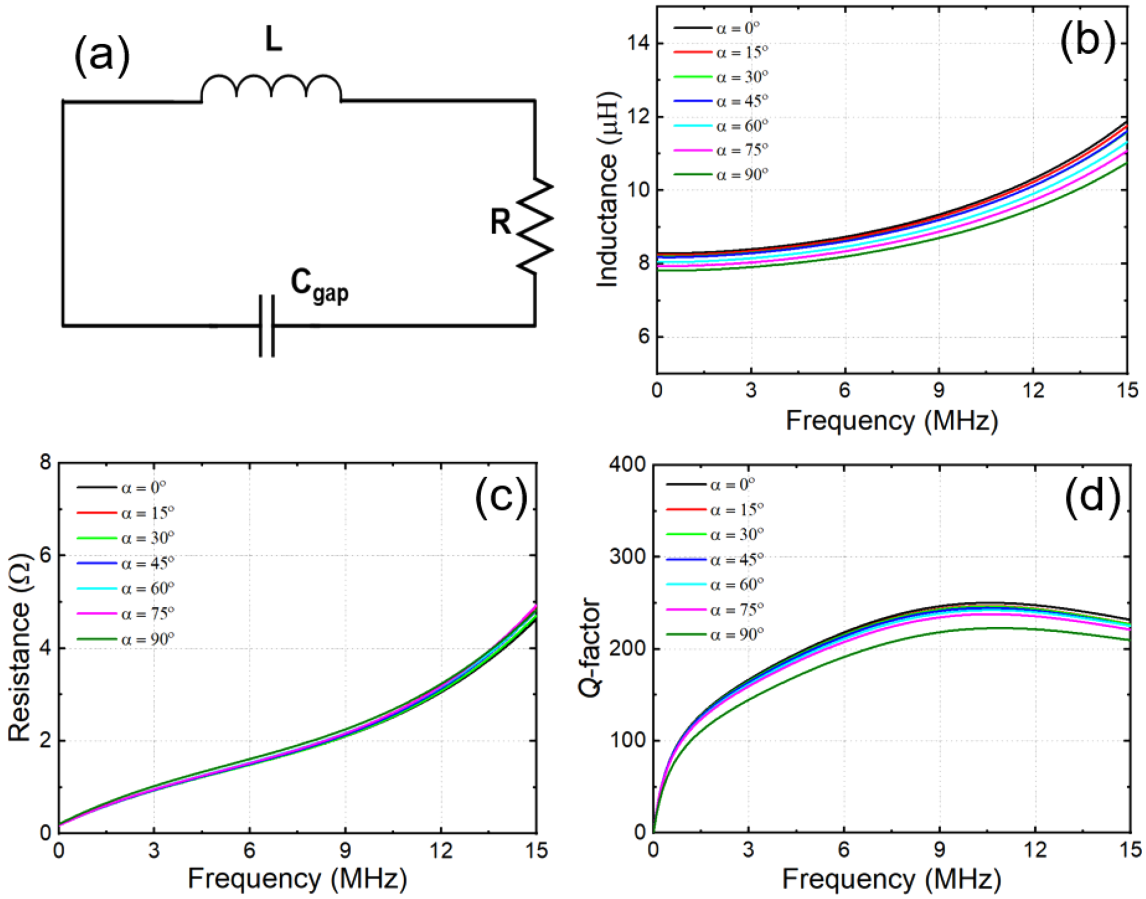

Fig. 3. (Color online) (a) Equivalent circuit of the resonator coil, (b) inductance, (c) resistance, (d) *Q*-factor of resonator coil under bending conditions.

the WPT system. The response of resonator coils to the bending is a property that needs to be investigated. Figure 2(b) shows a schematic of a bending resonator coil with bending angle α. The angle α is formed by two lines connecting from the center of the arc formed by the resonator coil (O) to the two points that are the center of the spiral (M) and the outermost point of the spiral (N). At the configuration of a flat resonator, point O goes to infinity, leading to angle α approaching 0°.

The resonator coil in WPT system can be modeled as an equivalent *RLC* circuit, as shown in Fig. 3(a). The internal parameters of the resonator coil, such as the series resistance, self-inductance, and self-capacitance, are expressed by R, L, and C_{gap}, respectively. When the external capacitor is soldered, it is considered to be connected parallel to the internal capacitor of the spiral, thereby reducing the resonant frequency of the resonator coil. The system to characterize the resonator coil can be represented as a one-port network. Therefore, the properties of the resonator can be expressed in terms of network parameters such as *S*, *Z*, *Y*, and *ABCD* [33]. From the definition of *Z*-parameters, the input impedance of the resonator coil is given by:

$$Z_{in} = R + j\omega L + \frac{1}{j\omega C} \tag{1}$$

The input impedance of the coil can be calculated from the *S*-parameters:

$$S_{11} = \frac{Z_{in} - Z_0}{Z_{in} + Z_0} \rightarrow Z_{in} = Z_0 \frac{S_{11} + 1}{1 - S_{11}} \tag{2}$$

with Z_0 as the port impedance.

As the resonator coils in an inductive link are operated below the self-resonant frequency, *RL* model is sufficient to replace the *RLC* model [34]. Since the coil capacitance is assumed to be much smaller than the inductance, we can extract the self-inductance (L) and the resistance (R) of the coils by the following relationship:

$$L = \mathrm{Im}\left(\frac{Z_{in}}{\omega}\right) \tag{3}$$

$$R = \mathrm{Re}\left(Z_{in}\right) \tag{4}$$

The Q-factor of the resonator coil can be calculated from the inductance and resistance as:

$$Q = \frac{\omega L}{R} \tag{5}$$

Figures 3(b-d) show the resonator coil parameters which were obtained from S-parameter extraction versus the bending angle. Figure 3(b) shows the inductance of the resonator coil at the frequency range from 0 to 15 MHz. The inductance of the coil at the planar state corresponding to a bending angle of 0° is always greater than a bent state. At the frequency of 6.78 MHz, the inductance of the resonator coil at a bending angle of 0° is 8.85 µH. When the bending angle increases, the inductance gradually decreases to 8.28 µH at the bending angle of 90°. The decrease in inductance of the resonator coil was also obtained with square shape coils in previous studies [35]. The coil's inductance at 90° reduces by 6.4 % compared to the planar state. Therefore, the resonant frequency of the coil is changed slightly. However, the Tx and Rx are identical, so the WPT system still works stably. Figure 3(c) shows the coil's resistance with various bending angles. The total resistance of the coil includes DC resistance and AC resistance. Where DC resistance is 0.2 Ω and the AC resistance increases with frequency due to the skin effect and the proximity effect caused by closely coupled striplines. As shown in Fig. 3(c), the total resistance of the coil does not change much following the bending angle at the MHz frequency region. According to the inductance and resistance, the Q-factors of the coil at different bending angles are calculated, as shown in Fig. 3(d). When the bending angle increases, the inductance decreases while the resistance is almost the same, which reduces the coil's Q-factor. At the frequency of 6.78 MHz, the Q-factor reduces from 232 to 201 when the bending angle changes from 0° to 90°.

In a WPT system, the coupling factor of the two resonator coils is an important parameter that affects the system's performance. After investigating the properties of the resonator coil at bending states in the above section, we continue to investigate the mutual inductance of the two coils under the bending conditions. The mutual inductance (M) of the two coupled coils can be derived from the impedance matrix Z-parameter of a 2-ports network as [13]:

$$Z_{2-port} = \begin{bmatrix} R + j\omega L & j\omega M \\ j\omega M & R + j\omega L \end{bmatrix} \tag{6}$$

The $Z_{2\text{-port}}$ can be converted from scattering parameters obtained by Vector Network Analyzer (VNA) measurement. Figure 4(a) shows the mutual inductance of two resonator coils under the inward bending conditions (the configuration shown in Fig. 5(b)). When the bending angle increases from 0° to 90°, the mutual inductance increases from 0.28 µH to 0.42 µH. That can be explained by, in the inward bending mode, the effective distance between the resonator coils will be closed while the bend angle increases. In contrast, in the outward bending mode (the configuration shown in Fig. 5(c)), the mutual inductance decreases from 0.28 µH to 0.14 µH when the bending angle changes from 0° to 90°. This change in mutual inductance will lead to a change in the coupling coefficient between the two resonators and thus affect the overall performance of the WPT system. When the mutual inductance between two resonator coils is greater, there will be a correspondingly larger coupling coefficient, and the WPT system will

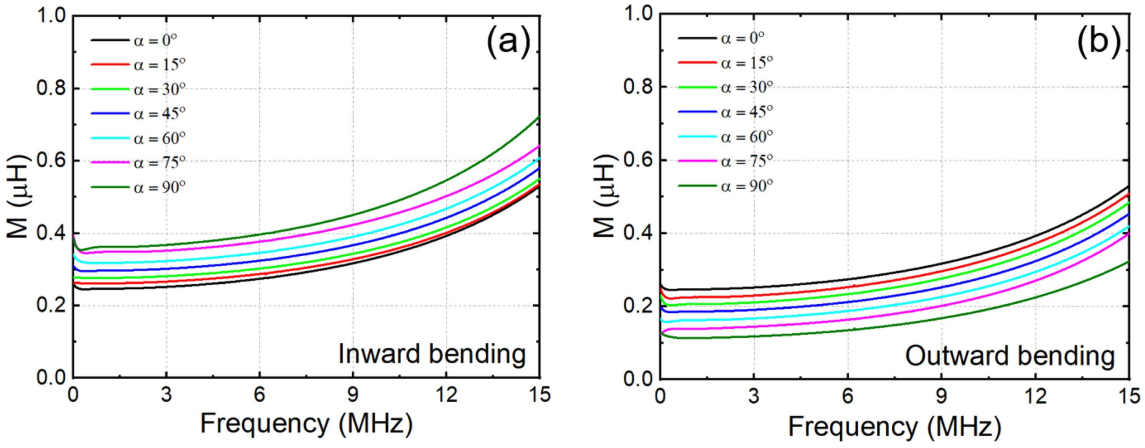

Fig. 4. (Color online) Mutual inductance of two resonator coils under various bending angles; (a) inward bending, (b) outward bending.

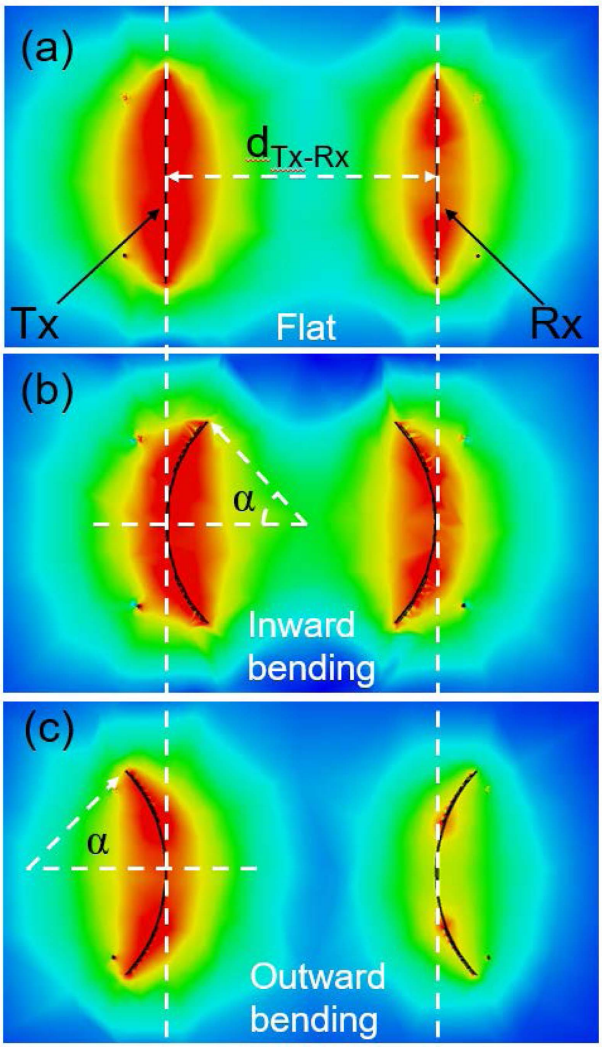

Fig. 5. (Color online) Field distribution in WPT system for three configurations; (a) flat resonator coils, (b) inward bending, (c) outward bending.

obtain better performance and vice versa with a smaller mutual inductance.

Electromagnetic (EM) simulations are performed to investigate the field distribution in WPT system at the resonant frequency of 6.78 MHz when the resonator coil is bent in both inward and outward cases. Figure 5(a) shows the magnetic field distribution around the original WPT system. A magnetic field is generated around Tx due to the resonant current flowing in the coil. The magnetic field strength tends to decrease at locations farther from Tx. However, at the position of Rx, the magnetic field strength increased quite large, although smaller than the Tx side. This proves that energy has been transferred from Tx to Rx through near-field interaction. Magnetic field strength on the Rx side is smaller than on the Tx side due to the Ohmic loss occurring at the Tx and Rx coils, which reduces the energy transfer efficiency. Figure 5(b) presents the field distribution of a WPT system when the resonator coil is inward bending with an angle of 45°. The result shows that the strength of the magnetic field at Rx is larger than the flat case. On the contrary, the magnetic field strength around the resonators has been reduced compared with the flat and inward bending case in the outward bending configuration, as shown in Fig. 5(c). The obtained results can be explained by: (i) bending coils reduce the magnetic field concentration on a flat cross-section; (ii) the effective distance bend d_{Tx-Rx} becomes smaller in the inward bending and larger in the outward bending case. The stronger or weaker magnetic field strength on the Rx side will improve or reduce the transfer efficiency of the WPT system.

3. Experiment Results

A MR-WPT system with flexible resonator coils was implemented to confirm the analysis in previous sections, as shown in Fig. 6. The system's configuration is similar to the analysis and simulation parts, as shown in Fig. 1, with the distance between two resonator coils is 200 mm. The Tx, Rx coils are fabricated by PCB technique on an FR-4 substrate with a thickness of 0.2 mm, thus minimizing fabrication errors and easily replicating. The FR-4 substrate is a rigid material with a large thickness, for example, above 1.6 mm. However, at a thin thickness of 0.2 mm, it becomes semi-flexible and can be easily bent with good elasticity. Thanks to such thin thickness, the Tx and Rx can be bent with angles from 0° to 90°. The resonant frequency of Tx and Rx is 6.78 MHz, which is tuned by

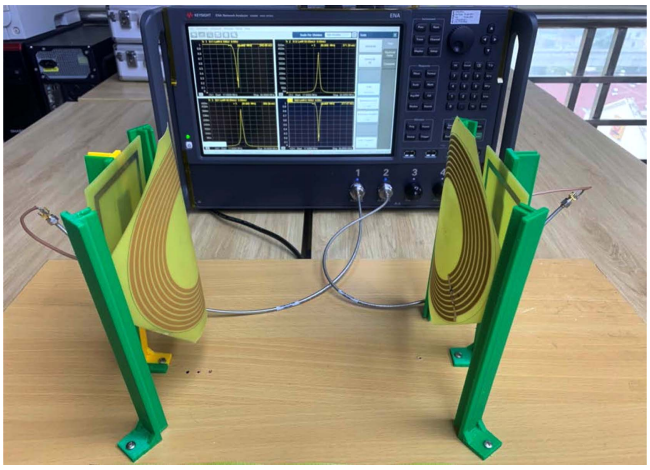

Fig. 6. (Color online) Experiment setup for the proposed WPT system with flexible resonator coils.

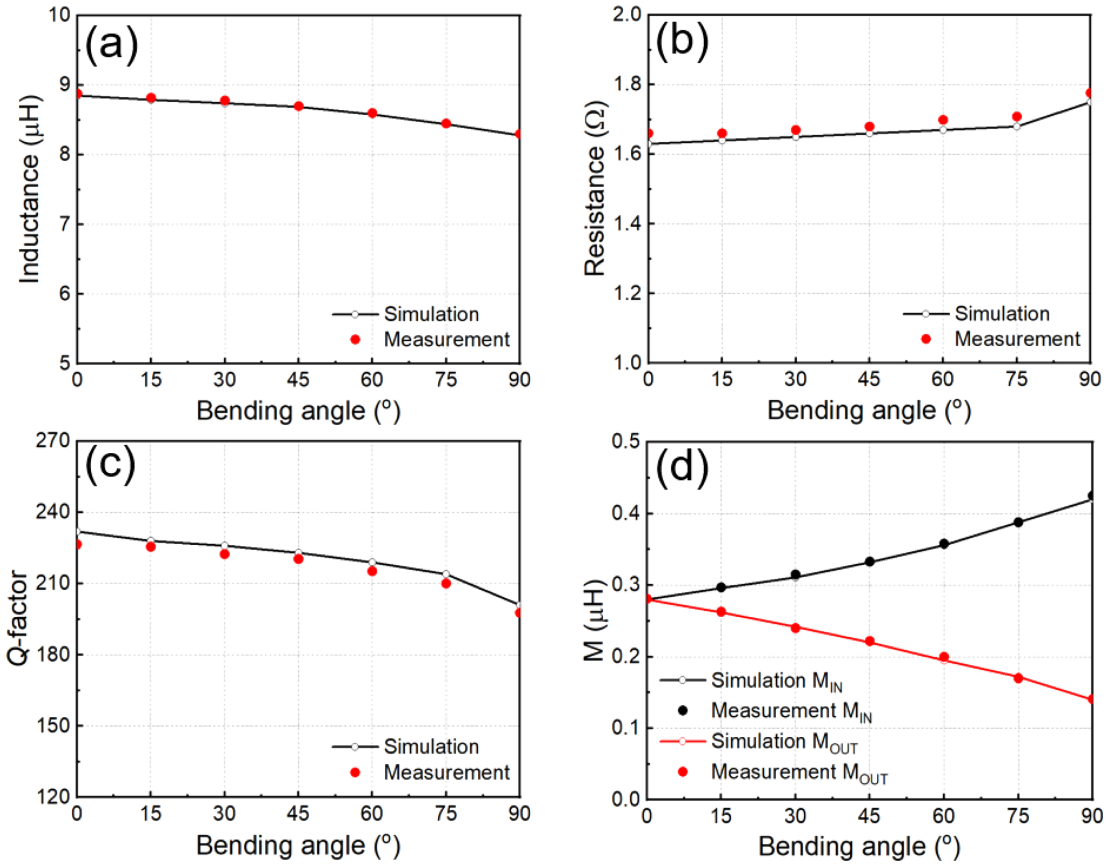

Fig. 7. (Color online) The comparison between simulation and measurement results of resonator coils under bending conditions; (a) inductance, (b) resistance, (c) *Q*-factor, (d) mutual coupling.

external capacitors. The characteristic of the WPT system is measured using the Vector Network Analyzer (Keysight ENA Network Analyzer E5080B 9 kHz-20 GHz) with a standard 2-port calibration technique. After removing the impedance mismatch by adjusting the distance from Tx and source loop (Rx and load loop), both S_{11} and S_{22} are less than -10 dB. Therefore the transfer efficiency of WPT system can be estimated using $|S_{21}|^2$ [36].

In order to validate the findings of the previous theoretical analysis, the parameters of the resonators, including inductance, resistance, Q-factor and mutual coupling under bending conditions, were measured and compared against the simulation results. The values of these parameters at the operating frequency of 6.78 MHz are illustrated in Fig. 7. Figure 7(a)-(c) shows the simulation and measurement results of coil's inductance, resistance and *Q*-factor under the bending angle from 0° to 90°. The results demonstrate that there is a strong correlation between the inductance values obtained from simulation and measurement. Meanwhile, the resistance value obtained from the measurement is slightly higher than that of the simulation (about 3 %). This can be explained by manufacturing and measurement errors. As a consequence of the variation in resistance values, the *Q*-factor of the resonator also undergoes a similar change with the resistance but in the opposite direction. Figure 7(d) shows the results of mutual inductance with two configurations of inward and outward bending, indicating a good agreement between simulation and measurement.

Figure 8 compares the measured efficiency of WPT system in different configurations, inward and outward bending with various angles. At the bending angle of 0° corresponding to the flat case, the transfer efficiency of WPT system was achieved at 60.5 %. The black curve depicts the efficiency of WPT system in the inward bending configuration. The efficiency improves from 60.5 % to 75.2 % when the bending angle increases from 0° to 90°. Although, the *Q*-factor of the resonator coils is reduced at bending. The mutual inductance between the two resonator coils is increased, leading to the system performance being improved. In the outward bending configuration, the efficiency drops from 60.5 % to 20.5 %

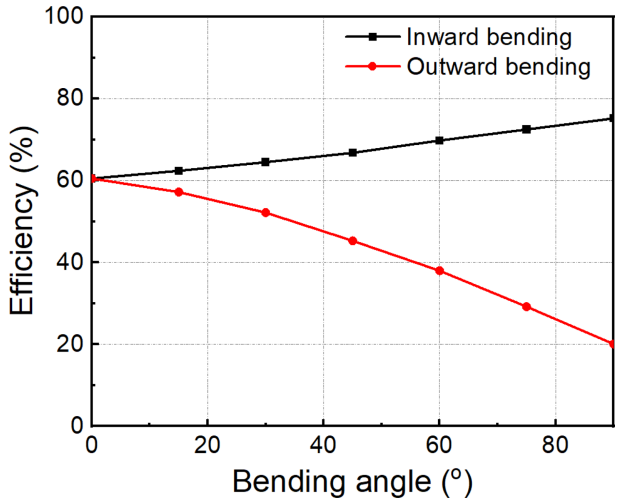

Fig. 8. (Color online) Measured efficiency of WPT system as a function of bending angle.

with the respective bending angles, as shown by the red curve. In this case, the efficiency degraded sharply due to both the *Q*-factor and mutual inductance being decreased. The measurement results are consistent with the field distribution simulations shown in Fig. 5.

Flexible resonator coils have potential applications in WPT, particularly in situations where traditional rigid coils would be impractical to use. The flexibility of the coils allows for easier integration into complex shapes and surfaces, making them suitable for a range of applications in complex electrical and electronics systems, such as wearable devices, IoT systems, or implantable medical devices. Additionally, the bending coils can improve the efficiency of WPT systems in some bending configurations. The size of the resonator coils may vary to suit specific applications, however, the same analysis can be used in the design. While a thin substrate can enhance flexibility and minimize the loss of resonator coils, it may result in a slight decrease in durability compared to a rigid substrate.

4. Conclusion

In this paper, we propose and analyze a MR-WPT system with flexible transmitter and receiver coils operating at MHz frequency. The changes in resonator coil properties, such as inductance, resistance, and *Q*-factor when subjected to bending, have been thoroughly investigated. In addition to the above parameters, the mutual inductance between the two bending resonator coils also affects the WPT performance. The field distribution obtained from EM simulation shows that the magnetic field strength increases in the inward bending and decreases in the outward bending configuration. The transfer efficiency improves from 60.5 to 75.2 % in the inward bending configuration due to the increase of mutual inductance even though the *Q*-factor of resonator coil is reduced. In the case of outward bending, both the *Q*-factor and mutual inductance decrease, so the efficiency of the WPT system is sharply reduced from 60.5 to 20.5 %. The study results can provide useful information for designing WPT systems applied to devices with non-planar transmitting and receiving surfaces, especially arc-shaped surfaces.

Acknowledgment

This work was supported by Hanoi University of Industry Research Fund under grant number 16-2022-RD/HĐ-ĐHCN.

References

[1] W. Adepoju, I. Bhattacharya, M. Sanyaolu, M. E. Bima, T. Banik, E.N. Esfahani, and O. Abiodun, IEEE Access **10**, 42699 (2022).
[2] K. Detka and K. Górecki, Energies **15**, 7236 (2022).
[3] M. Song, P. Belov, and P. Kapitanova, Appl. Phys. Rev. **4**, 021102 (2017).
[4] W. Liu, K. T. Chau, X. Tian, H. Wang, and Z. Hua, Renew. Sust. Ener. Rev. **180**, 113298 (2023).
[5] Y. Wang, Z. Sun, Y. Guan, and D. Xu, Proc. IEEE **111**, 528 (2023).
[6] M. Song, P. Jayathurathnage, E. Zanganeh, M. Krasikova, P. Smirnov, P. Belov, P. Kapitanova, C. Simovski, S. Tretyakov, and A. Krasnok, Nat. Electron. **4**, 707 (2021).
[7] M. Xia and S. Aissa, IEEE Trans. Signal Process. **63**, 2835 (2015).
[8] Y. Zeng, C. Lu, R. Liu, X. He, C. Rong, and M. Liu, IEEE Trans. Power Electron. **38**, 1440 (2023).
[9] E. Lee, W. Kang, and H. Ku, J. Electr. Eng. Technol. **14**, 2097 (2019).
[10] T. S. Pham, B. X. Khuyen, B. S. Tung, T. T. Hoang, V. D. Pham, Q. M. Ngo, and V. D. Lam, J. Electron. Mater. **50**, 443 (2021).
[11] S. Y. R. Hui, W. Zhong, and C. K. Lee, IEEE Trans. Power Electron. **29**, 4500 (2014).
[12] X. Wei, Z. Wang, and H. Dai, Energies **7**, 4316 (2014).
[13] Q. Chen, X. Zhang, W. Chen, and C. Wang, Sci. Rep. **12**, 19418 (2022).
[14] S.-Y. Kim, N.-R. Kwon, S.-H. Ahn, and W.-S. Lee, IEEE Trans. Antennas Propag. **71**, 4036 (2023).
[15] A. Kurs, A. Karalis, R. Moffatt, J. D. Joannopoulos, P. Fisher, and M. Soljačić, Science **317**, 83 (2007).
[16] D.-H. Kim and Y.-J. Park, Electron. Lett. **52**, 1321 (2016).

[17] A. Vallecchi, S. Chu, L. Solymar, C. J. Stevens, and E. Shamonina, IET Microw. Antennas Propag. **13**, 55 (2019).
[18] C. Lu, X. Huang, X. Tao, C. Rong, and M. Liu, IEEE Access **8**, 152900 (2020).
[19] L. Shi, N. Rasool, H. Zhu, K. Huang, and Y. Yang, IEEE Microw. Wirel. Compon. Lett. **30**, 705 (2020).
[20] D. M. Roberts, A. P. Clements, R. McDonald, J. S. Bobowski, and T. Johnson, IEEE Trans. Microw. Theory Tech. **69**, 3510 (2021).
[21] T. S. Pham, T. D. Nguyen, B. S. Tung, B. X. Khuyen, T. T. Hoang, Q. M. Ngo, L. T. H. Hiep, and V. D. Lam, Sci. Rep. **11**, 1 (2021).
[22] K. Sondhi, N. Garraud, D. Alabi, D. P. Arnold, A. Garraud, S. G. R. Avuthu, Z. H. Fan, and T. Nishida, J. Micromechanics Microengineering **29**, 084006 (2019).
[23] V. K. Bandari, Y. Nan, D. Karnaushenko, Y. Hong, B. Sun, F. Striggow, D. D. Karnaushenko, C. Becker, M. Faghih, M. Medina-Sánchez, F. Zhu, and O. G. Schmidt, Nat. Electron. **3**, 172 (2020).
[24] S. Jeong, J. Song, H. Kim, S. Lee, J. Kim, J. Lee, Y. Kim, S. Kim, and J. Song, in 2017 IEEE Wirel. Power Transf. Conf. WPTC (2017), pp. 1-3.
[25] M. Bissannagari, T.-H. Kim, J.-G. Yook, and J. Kim, Nano Energy **62**, 645 (2019).
[26] Y. Li, N. Grabham, R. Torah, J. Tudor, and S. Beeby, Appl. Sci. **8**, 912 (2018).
[27] S. Jeong, T.-W. Kim, S. Lee, B. Sim, H. Park, K. Son, K. Son, S. Kim, T. Shin, Y.-C. Kim, J. Kim, and B.-J. Kim, IEEE Trans. Compon. Packag. Manuf. Technol. **12**, 1748 (2022).
[28] L. T. H. Hiep, B. X. Khuyen, B. S. Tung, Q. M. Ngo, V. D. Lam, and T. S. Pham, Materials **15**, 6583 (2022).
[29] K. Rajaram and J. Kim, Nano Energy **57**, 317 (2019).
[30] D. Xu, Q. Zhang, and X. Li, Sustainability **12**, 4149 (2020).
[31] W. Lee, and Y.-K. Yoon, Sensors **23**, 1972 (2023).
[32] H. Kim, S. Yoo, H. Joo, J. Lee, D. An, S. Nam, H. Han, D.-H. Kim, and S. Kim, Sci. Adv. **8**, eabo4610 (2022).
[33] D.-W. Seo, J.-H. Lee, and H. S. Lee, ETRI J. **38**, 568 (2016).
[34] B. Lenaerts and R. Puers, Omnidirectional Inductive Powering for Biomedical Implants (Springer Netherlands, Dordrecht, 2009).
[35] H. Wang, M. Totaro, S. Veerapandian, M. Ilyas, M. Kong, U. Jeong, and L. Beccai, Adv. Mater. Technol. **5**, 2000659 (2020).
[36] A. L. A. K. Ranaweera, T. P. Duong, and J.-W. Lee, J. Appl. Phys. **116**, 043914 (2014).